This full text paper was peer reviewed at the direction of IEEE Communications Society subject matter experts for publication in the ICC 2007 proceedings.

Detection of Frequency-Hopped Waveforms Embedded in Interference Waveforms with Noise

John Weber, Kyle Kowalske, Clark Robertson, Frank Kragh, and Christopher Brown

***Abstract*—Bandwidth usage has become more complex such that it is not uncommon that multiple signals of appreciable power may be present within the same bandwidth. The presence of multiple signals in addition to additive white Gaussian (AWGN) increases the difficulty of detecting frequency-hopped (FH) waveforms. This paper investigates the performance of an exponential-averaging based FH detection method in the presence of interfering signals and AWGN. The detection method provides an estimate of the noise plus inference spectrum using exponential averaging and then generates an estimate of the desired signal spectrum by combining the estimated noise plus interference spectrum with the composite (desired signal plus interference plus noise) spectrum. Finally, this paper evaluates the detector's performance as a function of the exponential coefficient, the combining method (division or subtraction), signal-to-AWGN ratio (SNR), and signal-to-interference ratio (SIR).**

***Index Terms*—Detection, estimation, frequency-hopped, exponential averaging.**

I. Introduction

The additional robustness of using frequency-hopping (FH) over non-FH signals in an interference environment makes FH signals well suited for use in frequency bands that contain multiple signals [1]. The presence of interference signals in addition to additive white Gaussian noise (AWGN) increases the difficulty of detecting a FH signal. FH detection methods are dependant on the amount of a priori knowledge of the channel, the interference signals, and the FH signal. In the case of perfect knowledge of the previous three factors, an optimum detector can be constructed. Since this is rarely the case, alternate approaches are required.

This paper investigates the recovery of a FH signal in the presence of wideband interference signals and AWGN. The a priori knowledge assumed in this paper is that the noise is AWGN, the interfering signals are high power wideband signals relative to a FH bin bandwidth, the FH signal is bounded within a given bandwidth, and the FH sequence is fixed for an entire search cycle. A general description of the exponential averaging FH detector is presented in Section II. In Section III, the signal, interference, and noise are discussed as well as the signal-to-AWGN (SNR) and signal-to-interference ratio (SIR) metrics. The simulation methods and results are presented in Section IV. The performance of the exponential averaging FH detector is displayed as a graph of probability of detection P_d versus SIR for a fixed value of SNR and probability of false alarm P_f. This paper expands on the work in [2] by including AWGN in addition to the interference signals, by improving the initial conditions used by the exponential averaging algorithm, by including the scaled subtraction combination method, and by evaluating the detector's performance with respect to P_d via simulations.

II. Exponential Averaging FH Detector

Exponential averaging is used to generate a spectral estimate of the AWGN plus the interference. The digitized signal is separated into smaller data segments, and the segments are transformed to the frequency domain using the discrete Fourier transform (DFT), weighted according to their order. The DFT of a segment is

$$X(k) = \sum_{n=0}^{N-1} x(n) \exp\left[-j\left(2\pi/N\right)nk\right],\ k = 0,1,...,N-1 \qquad (1)$$

where N is the number of samples and $x(n)$ is the sampled data [3]. The detection process is expressed analytically as

$$M(k) = \sum_{i=1}^{L} \alpha^{L-i} Y_i(k) \qquad (2)$$

where $M(k)$ is the AWGN plus interference spectral estimate, α is a weight factor which has values ranging from zero to one, L is the number of segments that the data is separated into, and $Y_i(k) = \left|X_i(k)\right|^2$ is the magnitude squared of the i^{th} segment DFT.

The spectral estimate of the FH signal is obtained by combining $M(k)$ with the composite (desired signal, interference, and noise) spectrum. The two combining methods used in this paper are scaled subtraction combining and quotient combining. The combining methods use element-by-element operations with respect to the frequency bins. The FH signal spectral estimation process using quotient combining is expressed analytically as

$$\tilde{Y}_q(k) = \sum_{i=1}^{L} Y_i(k) / M(k). \qquad (3)$$

The FH signal spectral estimation process using scaled

Report Documentation Page

Form Approved
OMB No. 0704-0188

1. REPORT DATE	2. REPORT TYPE	3. DATES COVERED
2007		**00-00-2007 to 00-00-2007**

4. TITLE AND SUBTITLE	5a. CONTRACT NUMBER
Detection of Frequency-Hopped Waveforms Embedded in Interference Waveforms With Noise	5b. GRANT NUMBER
	5c. PROGRAM ELEMENT NUMBER
6. AUTHOR(S)	5d. PROJECT NUMBER
	5e. TASK NUMBER
	5f. WORK UNIT NUMBER
7. PERFORMING ORGANIZATION NAME(S) AND ADDRESS(ES) **Department of Electrical and Computer Engineering,Naval Postgraduate School ...,Monterey,CA,93943**	8. PERFORMING ORGANIZATION REPORT NUMBER
9. SPONSORING/MONITORING AGENCY NAME(S) AND ADDRESS(ES)	10. SPONSOR/MONITOR'S ACRONYM(S)
	11. SPONSOR/MONITOR'S REPORT NUMBER(S)

12. DISTRIBUTION/AVAILABILITY STATEMENT
Approved for public release; distribution unlimited

13. SUPPLEMENTARY NOTES
See also ADM002055. Proceedings of the 2007 IEEE International Conference of Communications (ICC 2007) Held in Glasgow, Scotland on June 24-28, 2007. U.S. Government or Federal Rights License

14. ABSTRACT

15. SUBJECT TERMS

16. SECURITY CLASSIFICATION OF:			17. LIMITATION OF ABSTRACT	18. NUMBER OF PAGES	19a. NAME OF RESPONSIBLE PERSON
a. REPORT **unclassified**	b. ABSTRACT **unclassified**	c. THIS PAGE **unclassified**	**Same as Report (SAR)**	**6**	

subtraction combining is expressed analytically as

$$\tilde{Y}_s(k) = \sum_{i=1}^{L} Y_i(k) - \beta M(k) \tag{4}$$

where β is a scaling factor and the operation is implemented element-by-element with respect to *k*. The scaling factor β is used to normalize $M(k)$ with respect to the average values of $Y_i(k)$ and is given by

$$\beta = \left(\sum_{i=0}^{L-1} \alpha^i \right)^{-1} = \frac{1-\alpha}{1-\alpha^L} \approx 1-\alpha. \tag{5}$$

The reciprocal of β is the geometric series, so the approximation for β is exact as *L* approaches infinity. The scaling factor β can also be included in quotient combining as a normalizing factor.

Describing the nature of the exponential averaging FH detector is more objective than describing how the parameters α, *N*, and *L* are selected. The primary method used for selecting the parameters is trial and error based on simulation results. However, a brief discussion of exponential averaging and the interrelation of *N* and *L* does provide some intuitive sense from which to subjectively address the selection of α, *N*, and *L*.

The spectral average of a series of sample sets from the same random process will tend to produce a smooth shape as the number of sample sets increases. This result is fairly intuitive in that the underlying spectrum of the random process tends to become more self evident as more data is averaged. Thus, it is not intended as a noise reduction method in and of itself since the noise is not reduced but rather smoothed.

In the event that a signal is not present during a portion of the period over which the average is taken, that signal's spectra will *not* be as strongly represented as compared to how it otherwise would have been represented if the signal was continuously present. FH signals are just such signals. Thus, if a spectral averaging process is used to estimate the spectrum from a composite signal which includes a FH signal, then the FH signal is suppressed. The amount that the FH signal is suppressed is related to the hop rate and the period over which the average is taken. As an example, if the averaging period is less then the FH sequence cycle, then a number of the frequency hops may be completely unrepresented in the spectral estimate.

The discussion above implies linear averaging, which equally weights all elements. Exponential averaging weights more recent elements more heavily. Thus, exponential averaging provides a convenient method to retain the benefits of averaging and has the potential to suppress signals with a time varying spectrum. The parameter α determines how heavily recent elements are weighted in the exponential average. A few factors that help determine what α should be are the amount of data that is available for processing, the duration of the FH hop cycle, and the duration of a full cycle for the interference signal. The parameter α should be chosen such that the spectrum of the FH signal appears time varying. Thus, by the time a hop is represented in a segment its previous representation is negligible in $M(k)$. Similarly, the factors used to determine α are also used to determine what values should be chosen for *N* and *L*.

The values of *N* and *L* are somewhat less arbitrary. The values of *N* and *L* are inversely proportional, assuming that the data segments are not zero padded. This assumption then implies that the segment size and *N* are equal. The value of *N* has an upper bound of the data length and a more practical upper restriction due to errors that result from exceeding machine memory. The value of *N* has a lower bound due to required frequency resolution. As an example, for most applications a 64 point DFT to evaluate a 10 MHz bandwidth is insufficient. Finally, the value of *N* should be chosen to be an integer power of two. This allows the DFT to be evaluated using a fast Fourier transform (FFT) without requiring zero padding.

In general it is better to choose smaller values of *N* within the range previously discussed. The reason that a smaller segment size is desired is that it reduces the chance that a segment contains multiple hops and, thus, increases the suppression of the FH signal by the exponential averaging. Once the value of *N* is determined, then the value of *L* is the integer number of times that *N* goes into the data length. Data that does not make up a complete sample set can either be disregarded or zero padded and used.

III. Signals and Metrics

The FH signal used to evaluate the two detection methods discussed in this paper is a FH minimum-shift keyed (MSK) waveform with seven frequency hops. The carrier frequency is 10 MHz. The FFT of the FH signal is shown in Fig. 1. The interference signal is the sum of a binary phase-shift keyed (BPSK) signal and a continuous wave (CW) signal. There are 21 CW signals in the bandwidth of interest. The FFT of the interference signal is shown in Fig. 2. The signals are sampled at 50 MHz. The BPSK signal is selected because of its relatively flat spectrum near the center of the main lobe. The CW signal was selected for its narrowband characteristic which is similar to a tone jamming signal. Tone jamming can be the most effective noise jammer to FH systems [4]. Since the two interference signals are dissimilar, the combination of the two signals summed with AWGN is a reasonably hostile environment in which to evaluate the detector. Visually, it is clear that if Fig. 1 and Fig. 2 are superimposed onto each other, it would be difficult to find the FH/MSK signal.

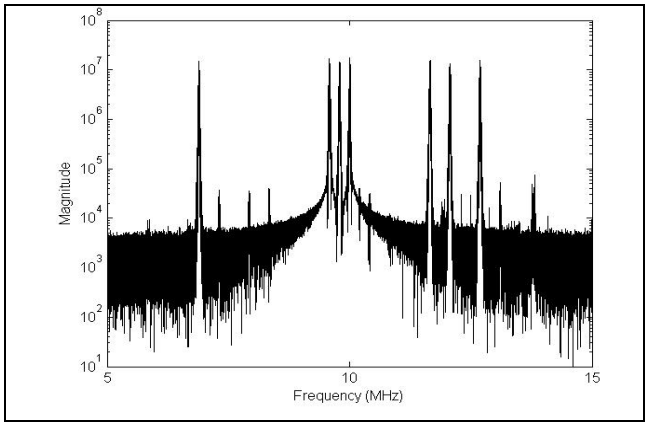

Fig. 1. Fourier transform of FH/MSK signal.

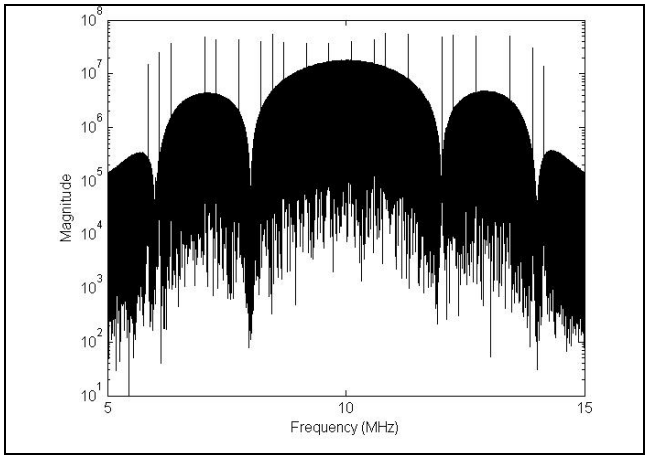

Fig. 2. Fourier transform of interference signals (BPSK and CW).

The performance metrics are SIR, SNR, and P_d. The signal power in SIR and SNR is the power in the FH/MSK signal. The interference power in SIR is the power of the BPSK and CW signals summed in the time domain. The noise power in SNR is the power in the AWGN. The values of SIR and SNR are varied by scaling normalized time domain signals. The metric P_d is estimated by simulation, dividing the number of detections by the number of simulations runs.

IV. Simulation Methods and Results

The simulations are generated in MATLAB. The FH/MSK, BPSK, and CW signals contain 1,032,192 samples. Since the sampling frequency is 50 MHz, the duration of each signal is approximately 20 ms. The *fft* function in MATLAB is used to compute the spectrum. The input data size used in the *fft* function is generally set to integer powers of two. For the simulations, a minimum spectral resolution of 24 kHz is assumed. This assumption sets the minimum number of points in the FFT to 2,048. The minimum number of points in the FFT is used unless otherwise stated. The minimum spectral resolution assumption may be based on a priori knowledge of the modulation type, hop rate, and the minimum frequency spacing required for signal orthogonality. The search range selected for the simulations is from 0 to 25 MHz. The frequency hops of interest lie between 6 and 13 MHz. For this reason, the *x* axis of the figures displaying the frequency response is limited to 5 to 15 MHz even though the data is processed between 0 and 25 MHz.

A. Interference/Noise Spectrum Estimation

The interference plus AWGN spectrum estimate is generated using (2) and shown in Fig. 3. The spectrum is generated using a 24,576-point FFT. The 24,576 point FFT was used verses the 2,048 FFT so that Fig. 3 would better replicate Fig. 2, which was generated using a 1,048,576 point FFT. Although the different scaling of Fig. 2 and Fig. 3 does not show it clearly there is a magnitude difference between the spectrum in the two figures. The magnitude difference between the two figures is attributed to the negative SIR with which Fig. 3 is generated. The SIR and SNR are obtained by holding the FH signal amplitude constant and varying the interference and AWGN signals to obtain the desired SIR and SNR, respectively.

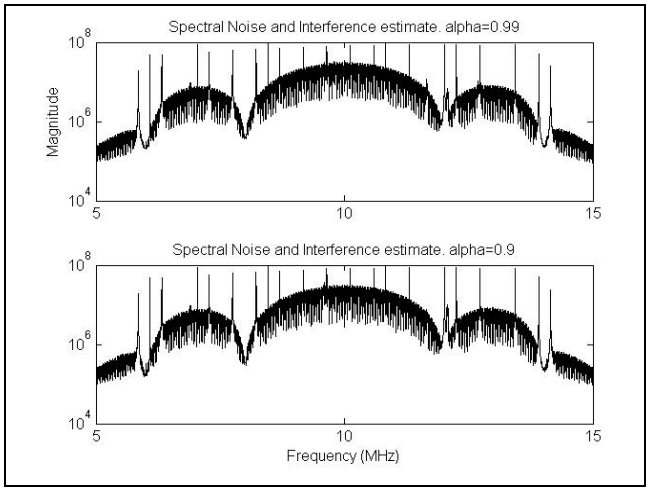

Fig. 3. Spectral interference estimate with $\alpha = 0.9$.

Two interference plus AWGN spectral estimates are shown in Fig. 3 to illustrate the influence of α on the estimate. The two most significant differences between the two estimates are the emerging spike at 11.7 MHz when $\alpha = 0.99$ and the slightly larger magnitude of the spike at 12.1 MHz when $\alpha = 0.9$. The two spikes are components of the FH/MSK signal. From these observations, it can be deduced that different values of α suppress components of the FH signal differently. A method for exploiting this conclusion is discussed in the next section.

B. FH Signal Spectrum Estimation

The variations in the suppression of the FH signal due to different values of α can be exploited using the two combining methods in (3) and (4). The results of the simulation shown in Figs. 4 and 5 provide some insight into how the two combining methods respond differently to differing values of α. In Fig. 4 the quotient combining method noise floor variance significantly increases for smaller

α. The numbers 1 through 7 in Figs. 4 and 5 show the hop order with 7 being the most recent hop.

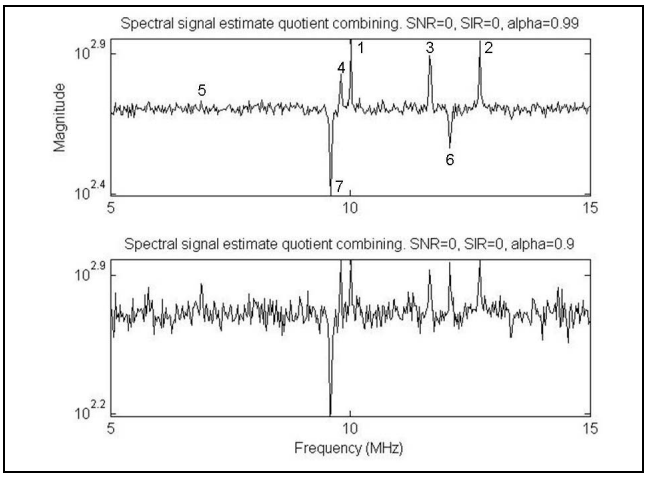

Fig. 4 Spectral FH signal estimate using quotient combining.

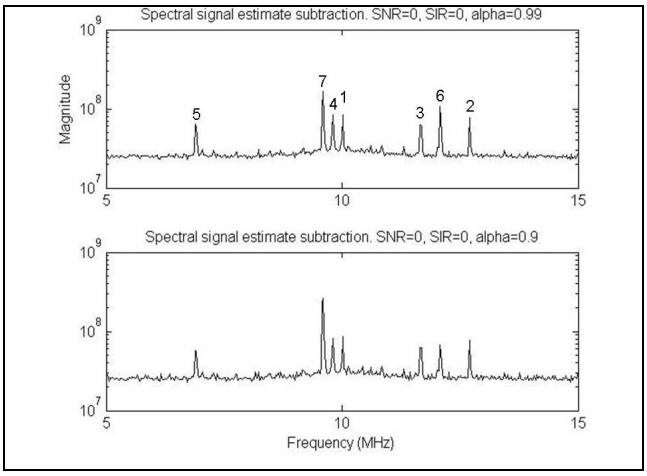

Fig. 5 Spectral FH signal estimate using scaled subtraction combining.

The earlier segments' contribution to the FH signal spectrum estimate is increased as α is increased within its range. This increase in earlier segment contribution improves the AWGN estimate and results in lowering the noise floor variance. However, the two combining methods' sensitivity to the lower noise floor variance differs. The quotient combining method is more sensitive to changes in the noise floor variance and, thus, requires a larger α to maintain a certain performance level. The subtraction combining method is less sensitive to the perturbation and has similar performance levels for the range $0.8 < \alpha < 1$.

This difference in sensitivity relegates the quotient combining method to values of α relatively close to one. Since the contribution of earlier segments increases as the value of α approaches one, more segments are needed the closer α is to one. This result indicates that the quotient combining method requires more segments than the scaled subtraction method. As the SIR and SNR are lowered, however, the quotient combining method outperforms the scaled subtraction combining method, as shown in Table I and Table II. The values in the tables are generated using single simulations and are presented as performance guidelines vice performance measures since they do not include any probabilistic measures.

TABLE I

The number of frequency hops detected by the exponential averaging FH detector given a 7 hop FH/MSK signal, quotient combining, and the respective SNR and SIR.

SNR dB (across) SIR dB (down)	0	-3	-6	-9	-12
0	6	6	6	6	5
-3	6	6	6	6	4
-6	6	6	6	5	4
-9	6	6	5	5	3
-12	4	4	4	4	2
-15	3	3	2	2	1
-18	1	1	0	0	0

TABLE II

The number of frequency hops detected by the exponential averaging FH detector given a 7 hop FH/MSK signal, scaled subtraction combining, and the respective SNR and SIR.

SNR dB (across) SIR dB (down)	0	-3	-6	-9	-12
0	7	7	7	7	2
-3	7	7	7	7	2
-6	7	7	5	3	1
-9	5	4	3	2	0
-12	2	1	1	1	0

Before describing the performance measures one other difference between the two combining methods should be discussed. Hops in the quotient combining method consist of both maxima and minima whereas hops in the scaled subtraction combining are exclusively maxima. The reason for the two extremes in quotient combining is that the hops that are poorly suppressed in the AWGN plus interference spectral estimate are repeatedly compared to segment spectrums where that particular hop is not present. This produces a minimum value in the signal spectral estimation. This also explains why there are only 6 hops detected verses 7. The obscured hop is the mid-hop transition point between the effectively suppressed hops and the poorly suppressed hops.

C. Decision Criteria

It is desirable that the performance measures that are selected will optimize the detector's performance. The detector is not the optimum detector since there is limited a priori knowledge. However, the decision criteria that the detector uses to evaluate the data can be optimized with respect to the detector. What is meant by optimum decision criteria is that P_f does not exceed a preset value and that P_d is maximized. The threshold is obtained using

$$P_f = \int_{V_t}^{\infty} f_x(x)dx \qquad (6)$$

where *x* is the random variable (RV) that is the input into the detector comparator when only noise (undesirable signals) are present, $f_x(x)$ is the probability density function of the RV x, and V_t is the threshold [1]. An analytic expression for $f_x(x)$ for scaled subtraction combining was sought by taking the inverse Fourier transform of the product of the noise and

interference characteristic functions and then applying the central limit theorem [5]. Since the summed RVs were not demonstrated to be independent as required by the central limit theorem, a simulation based estimate of the probability density function was constructed.

To narrow the focus of the paper, and since quotient combining has performance advantages over scaled subtraction combining, the rest of the paper will primarily focus on quotient combining. The number of points in the simulation FFT is set to 2,048. Thus, there are 1,024 frequency bins that correspond to frequencies from 0 to 25 MHz. The output from each one of these bins is considered a RV, and their distribution must be known to set the decision criteria.

The simulation based estimate of the probability density function for the individual frequency bins, given quotient combining, is well modeled by a Gaussian distribution as shown in Fig. 6. The mean is 504 and the variance is 14.5. The probability density function is consistent for noise-to-interference ratios from 18 dB to -18 dB throughout the spectrum. The threshold was set to 3.5 standard deviations above the mean. The resulting P_f is 0.0002. The simulation based false alarm error ratio is 0.0005. The false alarm ratio is generated from over a quarter of a million simulations where each simulation processed over a million data points.

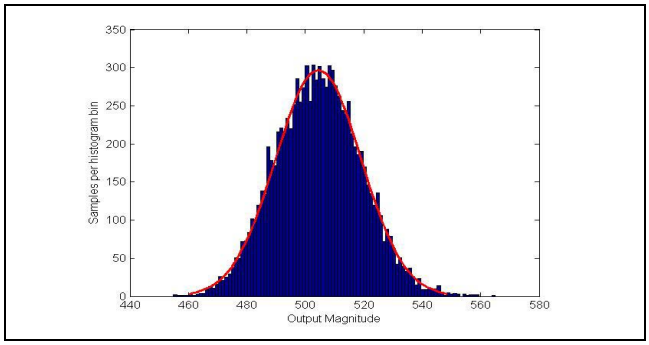

Fig. 6 Gaussian estimate (line) and histogram of a single frequency bin component within the AWGN plus interference spectral estimation.

Before the threshold can be applied, the FH signal's effect on the distribution should be understood. The effect of a hop on a frequency bin's distribution varies depending on whether the hop is detected as a minimum or a maximum. If the hop is detected as a maximum, then the mean is positively shifted. When the hop is detected as a minimum, the mean is negatively shifted. Thus, the threshold must be used at both positive and negative values to ensure that both maxima and minima hops are detected. This doubles the value of P_f and closes the gap between the theoretical and the measured result.

D. Simulation Results

The simulation results are presented in graphs of the detector's performance for each specific hop. The graphs plot estimated P_d verses SIR for a fixed SNR. The hops are numbered according to their temporal order as indicated in previous figures. Hop number 5 was not included since its estimated P_d is less than 0.01. The P_d estimates are based on simulations that cycled 5,000 times. To cover the exponential averaging detector's effective range of performance, the SNR values are -3 dB, -9 dB, and -15 dB.

The simulation results when the SNR equals -3 dB shows the general trend that the number of hops that are detectable is reduced as SIR decreases as shown in Fig. 7. The order at which specific hops are obscured from detection is a combination of the local SIR at the hop frequency, the SNR, and the temporal hop order where the mid-hops are more obscured. Hop number five is the mid-transition hop and is obscured from detection. In an SIR dominated environment, the temporal hop order and local SIR at the hop frequencies predominantly determine the order at which specific hops are obscured. The frequency hop with the lowest local SIR is hop four with hops one and seven a fraction of a dB higher, hops two, three, and five about 6 dB up, and hop six 10 dB up, as shown by Figs. 1 and 2.

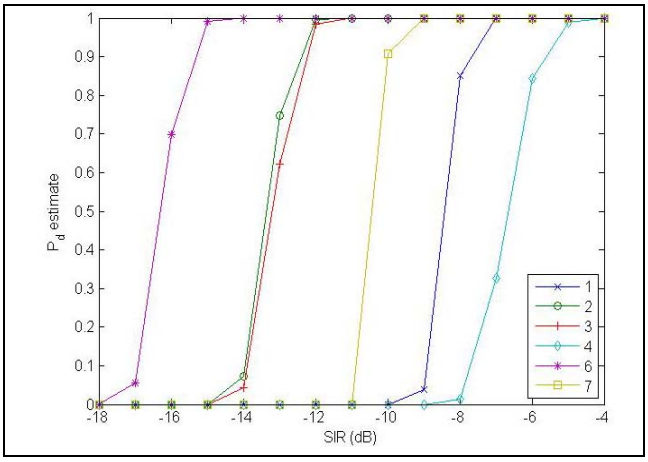

Fig. 7 Estimated P_d verses SIR with an SNR equal to -3 dB for 6 of the 7 hops using an exponential averaging FH detector with quotient combining.

Based on the local SIR and temporal order, the first hop expected to be obscured from detection is hop-four; however, as discussed previously, the mid-transition hop (hop five) is obscured from detection first. Thus, the temporal order of hops obscured is shifted to more recent temporal mid-hops. Hop four is the next hop to be obscured from detection, followed by hops one and seven as a result of the local SIR. The more recent end-hop, hop seven, has a one dB performance advantage, over the earlier end-hop hop one showing the emphasis of the *recent* end-hop. At low SIR relative to the SNR, the detector's performance with hops two and three is dominated by the SIR as compared to the one dB performance difference shown by the hop order influence with hops one and two. Note that the relative performance between hop four and hops two and three is approximately 6 dB, which corresponds to the local SIR difference between the hops. The last hop to be obscured from detection is hop six, which is 9 dB down from hop four. This closely corresponds to hop-six being 10 dB down from hop-four with respect to the local SIR. The abrupt change in the estimated probability of detection for specific hops is indicative of a jamming environment or, equivalently, an environment where the influence of SIR versus SNR dominates the detector's performance.

The simulation result when the SNR = -9 dB further supports the general trend that the number of hops that are detectable is reduced as SIR decreases as shown in Fig. 8. The increased influence of SNR on the detector's performance is shown by the less abrupt change of the estimated probability of detection for hops two, three, four, and six in Fig. 8. The detector's better performance with end-hops versus mid-hops as the significance of SNR increases over SIR is illustrated by the performance differences between hops two and three in Figs. 7 and 8. The minimum influence of SNR on the detection of hops one and seven is shown by the similar abrupt change in the estimated probability of detection in Figs. 7 and 8. These observations indicate that the relation between the hop order and the detector's performance increases as SNR increases relative to SIR.

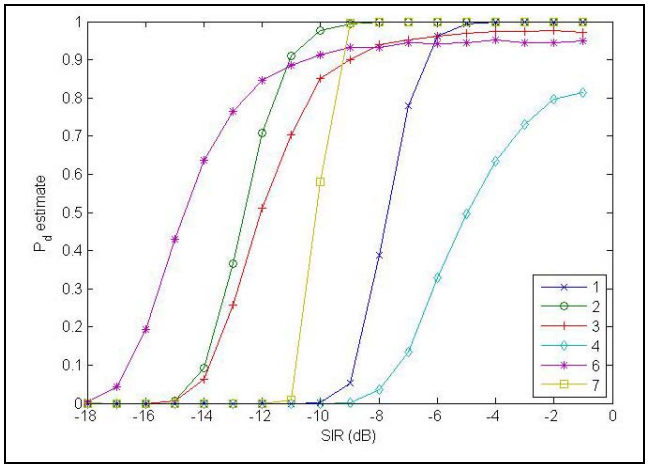

Fig. 8 Estimated P_d verses SIR with an SNR equal to -9 dB for 6 of the 7 hops using an exponential averaging FH detector with quotient combining.

The simulation result when SNR = -15 dB shows the general trend that the number of hops that are detectable is reduced as SIR is decreased, as shown in Fig. 9. The dominant influence of SNR versus SIR with respect to the detector's performance is shown by the gradual change in the estimated probability of detection for all hops in Fig. 9. The relation of the detector's better end-hop versus mid-hop performance as SNR increases relative to SIR is further supported by the detector's better performance with end-hops one, two, and seven as compared to mid-hops three and six, as shown in Fig. 9. The performance results when SIR is dominate shown in Fig. 7, provide a limiting performance measure for decreased SNR illustrated in Figs. 8 and 9. Finally, no relationship is observed between the estimated probability of detection for a specific hop and the hop's proximity to a CW signal for any of the simulations when SNR equals -3, -9, and -15 dB.

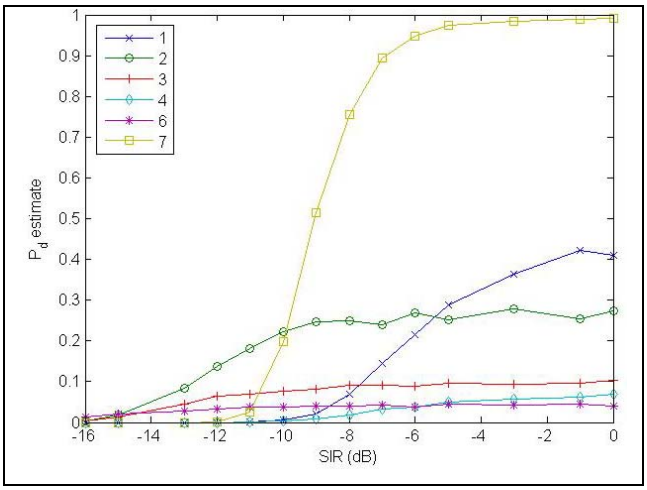

Fig.. 9 Estimated P_d verses SIR with an SNR equal to -15 dB for 6 of the 7 hops using an exponential averaging FH detector with quotient combining.

V. Conclusion

An exponential averaging based FH detector and its performance is discussed. The performance is evaluated with a FH/MSK signal embedded in interference waveforms and AWGN. The detector's description includes how the detector estimates the interference and noise spectrum, how the detector estimates the FH signal spectrum, and how the decision criteria is developed and implemented. The performance of the detector for various SNR and SIR is shown in Tables I and II and Figs. 7 through 9. In general, when either SNR or SIR is -15 dB or lower, the detector's performance is significantly degraded.

Future work could include theoretically evaluating the probability density function of the RV that models the input to the comparator so that a theoretical P_d and P_f can be evaluated, establishing the hop order based on the knowledge of which hop is obscured, and evaluating the algorithm for a fading channel.

References

[1] J. G. Proakis, *Digital Communications*, New York, NY. McGraw-Hill, 2001, pp. 771-783.

[2] C. Brown, K. Kowalske, and C. R. Robertson, 'Detection of Frequency-Hopped Waveforms Embedded in Interference Waveforms," *IEEE MILCOM,* pp. 747-753, 2005.

[3] R. D. Strum, and D. E. Kirk, *First Principles of Discrete Systems and Digital Signal Processing,* Reading, MA., Addison-Wesley, 1989, pp. 367-387.

[4] R. L. Peterson, R. E. Ziemer, and D. E. Borth, *Introduction to Spread Spectrum Communications,* Upper Saddle River, NJ. Prentice Hall, 1995, 327-374.

[5] A. Papoulis, and S. Pillai, *Probability, Random Variables and Stochastic Processes 4th ed*, Boston, MA., McGraw Hill, 2002, pp 152-164, 278-284.